Mesoscale Convective Systems over Southeastern South America and Their Relationship with the South American Low-Level Jet

PAOLA SALIO AND MATILDE NICOLINI

Centro de Investigaciones del Mar y la Atmósfera, CONICET/UBA, and Departamento de Ciencias de la Atmósfera y los Océanos, Universidad de Buenos Aires, Buenos Aires, Argentina

EDWARD J. ZIPSER

Department of Meteorology, University of Utah, Salt Lake City, Utah

(Manuscript received 13 October 2005, in final form 19 May 2006)

ABSTRACT

Prior studies have shown that the low-level jet is a recurrent characteristic of the environment during the initiation and mature stages of mesoscale convective systems (MCSs) over the Great Plains of the United States. The South American low-level jet (SALLJ) over southeastern South America (SESA) has an analogous role, advecting heat and moisture from the Amazon basin southward into the central plains of southeastern South America, generating ideal environmental conditions for convection initiation and growth into MCSs. This research has two purposes. One is to describe the characteristics of a 3-yr MCS sample in South America, south of the equator, and its related geographical distribution of convection frequency. The other is to advance the knowledge of the evolution of favorable environmental conditions for the development of large MCSs, specifically those that mature under SALLJ conditions. High horizontal and temporal resolution satellite images are used to detect MCSs in the area for the period 1 September 2000–31 May 2003. Operational 1° horizontal resolution fields from NCEP are used to examine the environment associated with the systems and for the same period. Differences between tropical and subtropical MCSs in terms of size, diurnal cycle, and duration are found. Tropical MCSs are smaller, shorter in duration, and are characterized by a diurnal cycle mainly controlled by diurnal radiative heating. Subtropical MCSs show a preference for a nocturnal phase at maturity over Argentina, which contrasts with a tendency for a daytime peak over Uruguay and southern Brazil. In all seasons, at least one subtropical MCS developed in 41% of the SALLJ days, whereas in the days with no SALLJ conditions this percentage dropped to 12%. This result shows the importance of the synoptic conditions provided by the SALLJ for the development of MCSs and motivates the study of the atmospheric large-scale structure that evolves in close coexistence between SALLJ and subtropical organized convection at the mature stage. The large-scale environment associated with large long-lived MCSs during SALLJ events over SESA evolves under thermodynamic and dynamic forcings that are well captured by the compositing analysis. Essential features are low-level convergence generated by an anomalous all-day-long strong low-level jet prior to the development of the system, overlapped by high-level divergence associated with the anticyclonic flank of the entrance of an upper-level jet streak. This provides the dynamical forcing for convection initiation in an increasingly convectively unstable atmosphere driven by an intense and persistent horizontal advection of heat and moisture at low levels. These processes act during at least one diurnal cycle, enabling gradual building of optimal conditions for the formation of the largest organized convection in the subtropical area. The frequency of convection culminates in a geographically concentrated nocturnal maximum over northeast Argentina on the following day (MCS–SALLJ day). The northeastward displacement and later dissipation of subtropical convection are affected by a northward advance of a baroclinic zone, which is related to horizontal cold advection and divergence of moisture flux at low levels, both contributing to the stabilization of the atmosphere.

Corresponding author address: Paola Salio, Centro de Investigaciones del Mar y la Atmósfera, Ciudad Universitaria, Pabellón II, 2do piso, 1428 Buenos Aires, Argentina.
E-mail: salio@cima.fcen.uba.ar

DOI: 10.1175/MWR3305.1

1. Introduction

Based on observational data and model analyses a number of papers have shown a northerly flow, located to the east of the Andes, is responsible for the significant transport of humidity and heat into the southeastern South American region (Nogués-Paegle and Mo 1997; Douglas et al. 1998; Paegle 2000; Nicolini and Saulo 2000; Salio et al. 2002; Marengo et al. 2002, 2004; Liebmann et al. 2004, among others). This region, usually referred to as southeastern South America (SESA), mostly covers the continental latitudes to the east of the Andes between 23° and 40°S and is identified by a box in Fig. 1. This northern flow is present throughout the year and shows an intense maximum during the spring (Berbery and Barros 2002; Vera et al. 2002; Campetella and Vera 2002; Berbery and Collini 2000). On some occasions the flow shows a low-level jet profile in its vertical structure favoring an intense horizontal transport of humidity at low levels of the atmosphere and, therefore, the transport of the momentum and humidity in the vertical structure, favoring the development of convection.

This flow, east of the Andes, often has a low-level jet profile and has been called the South American low-level jet (SALLJ) and has been studied by many authors (Marengo et al. 2004; Salio et al. 2002, among others). It has also been the focus of a field experiment called the South American Low-Level Jet Experiment (SALLJEX; Vera et al. 2006). In their analysis of a 15-yr period of the European Centre for Medium-Range Forecast (ECMWF) Re-Analysis (ERA-15), Salio et al. (2002) found that the SALLJ events, which extend south of 25°S generate the conditions of instability necessary for the development of convection in the subtropical area and explain 45% of the summer precipitation in the SESA region. Liebmann et al. (2004) show results coinciding with those found by Salio et al. (2002) for the strong SALLJ events, whereas, in the case of weak SALLJ events, increased precipitation in the South Atlantic convergence zone is observed. This convergence zone is a quasi-stationary region of enhanced convection that extends southeastward from the intertropical convergence zone anchored over the Amazon region toward the South Atlantic Ocean.

The question that arises, regarding the precipitation explained by the SALLJ events over the SESA region, is whether these events are capable of creating the environmental conditions conducive to the development of deep and organized convection, which include a close phase locking between convection and the low-level jet.

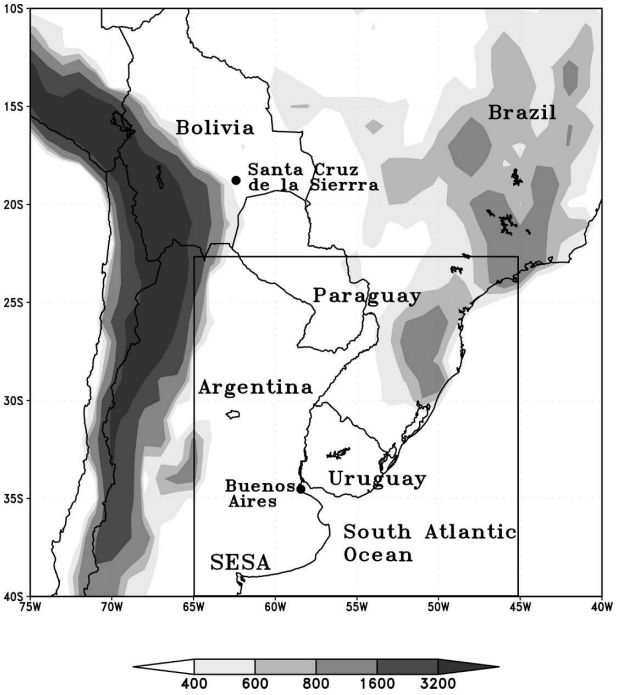

FIG. 1. Topography over South America. Contours correspond to terrain elevations of 200, 400, 800, 1600, and 3200 m.

Numerous authors have previously recognized the synoptic and mesoscale processes that precondition the environment and/or trigger convection. Johnson and Mapes (2001) have summarized these processes associated with severe convective weather and Fritsch and Forbes (2001) have documented the dynamic features and thermodynamic patterns present in the large-scale environment related to mesoscale convective systems (MCSs). One of the efficient subsynoptic mechanisms in destabilizing the atmosphere is provided by the presence of a low-level jet parallel to mountain ranges. Prior studies have shown that the low-level jet is a recurrent characteristic of the environment during the initiation and maturity of the mesosystems in the Great Plains of the United States (Maddox 1983; Cotton et al. 1989). In the Southern Hemisphere, Velasco and Fritsch (1987) and Nieto Ferreira et al. (2003) revealed the analogous role played by the maximum northerly flow, which favors the development of MCSs in subtropical latitudes in South America. Over SESA, these systems are characterized by their large size and intensity, by accounting for 60% of the precipitation (Mota 2003) and, in some instances, by generating severe phenomena in the area (Velasco and Fritsch 1987; Silva Dias 1999). Nicolini et al. (2002) compiled the environmental conditions in a sample of 27 heavily precipitating MCSs over SESA, and found a high correlation between these events and the occurrence of SALLJ

events extending south and penetrating into northern Argentina (81% of the 27 cases studied). Siqueira and Machado (2004) studied the relationship between tropical and subtropical convection with the displacement of frontal zones, showing the presence of a northerly flow before and during the formation of the convection in the subtropical area. Despite the consensus that there is a close relationship between the SALLJ and the development and maintenance of the MCSs, no systematic analysis of the evolution of the atmospheric circulation and organized convection has been carried out focusing on a situation when this relationship is occurring.

This research has two purposes. One is to describe the characteristics of a 3-yr MCS sample in South America, south of the equator, and its related geographical distribution of convection frequency. The other is to advance the knowledge of the evolution of favorable environmental conditions for the development of large MCSs, specifically those that mature under SALLJ conditions. High horizontal and temporal resolution satellite images are used to detect MCSs in the area for the period 1 September 2000–31 May 2003. Operational 1° horizontal resolution fields from the National Centers for Environmental Prediction (NCEP) are used to examine the environment associated with the systems and for the same period.

The paper is organized as follows. Section 2 describes the data and the methodology employed to detect MCS and SALLJ events. Section 3 shows the properties of the MCSs and their geographical and temporal distributions. In section 4, the evolution of frequency of convection for those days with both SALLJ and MCSs is shown. The environment of the subtropical MCSs associated with the SALLJ is shown in section 5, and the conclusions are summarized in section 6.

2. Data and methodology

To detect MCSs, IR brightness temperature was employed at half-hourly intervals with a horizontal resolution of 4 km over the area between 10°–40°S and 40°–75°W (Fig. 1) from 1 September 2000 to 31 May 2003. More information about the data can be obtained from Janowiak et al. (2001); and online at http://lake.nascom.nasa.gov/).

A convective system is defined as an area of at least 150 pixels (2400 km^2) enclosed by a temperature threshold. The threshold used in this paper is 218 K, in accordance with Machado et al. (1998) as representative of the presence of a deep-convection region. The clustering and the tracking technique called forecasting and tracking of active cloud clusters (FORTRACC) were employed to determine the life cycle of the systems. One cluster is defined as a contiguous region that verified the considered temperature threshold. The position and the evolution of each cluster in time are determined through a tracking algorithm to decide their continuity based on a maximum areal overlap on each successive image (Machado and Laurent 2004). The program detects when the system initiates from spontaneous generation and when it merges with another system or splits during its life cycle. This objective tracking was performed over the whole period of available images. A total of 12 979 systems were identified by FORTRACC in autumn (March–May), 2161 in winter (June–August), 13 904 in spring (September–November), and 22 640 in summer (December–February) without applying any criteria in regard to size or life span. Winters were excluded from this study because the number of systems that comply with the imposed criterion of the minimum size threshold is much smaller than the number encountered in the other seasons (Salio et al. 2004).

A definition of MCSs similar to that used by Cotton et al. (1989) and by Nicolini et al. (2002) was applied in order to study deep and organized convection in a sample of systems with features similar to those studied by other authors in different parts of the world. The initiation stage of the systems is defined when the area enclosed by the 218-K isotherm exceeds 50 000 km^2 (3125 pixels). The mature stage is attained when the above area reaches its maximum extent, whereas the dissipation stage is defined when the enclosed area crosses the 50 000 km^2 threshold again. A second brightness temperature threshold was not employed, because prior studies (e.g., Augustine and Howard 1988) found no significant differences in their results using two thresholds.

The MCSs generally undergo merging and splitting throughout their life cycles. Because it is difficult to determine the magnitude of environmental disturbance caused by the interaction of large systems, those systems that underwent merging or splitting for any length of time were further analyzed to avoid the possibility of any system extending beyond one life cycle. Thus, the sample is composed of numerous large systems that experience merging only with small systems, or do not split into two large systems. Likewise, those systems that have an area less than 50 000 km^2 for any length of time were eliminated in order to maintain a standard size throughout the entire life span.

The operational fields of the NCEP Global Data Assimilation System (GDAS) with horizontal resolution of 1° in latitude and longitude, 26 vertical levels, and 6-h temporal resolution are used to detect the SALLJ

TABLE 1. Number of SALLJ and NOSALLJ days detected during the different seasons of the year and number of SALLJ and NOSALLJ days where at least one MCS is detected considering its tropical or subtropical position.

Season	Day criteria	No. of days	No. of days where at least one MCS is detected	
			Tropical	Subtropical
Autumn	SALLJ	82 (10.0%)	14 (1.7%)	32 (3.9%)
	NOSALLJ	194 (23.7%)	31 (3.8%)	29 (3.5%)
Spring	SALLJ	107 (13.1%)	22 (2.7%)	47 (5.7%)
	NOSALLJ	166 (20.3%)	48 (5.8%)	14 (1.8%)
Summer	SALLJ	96 (11.7%)	28 (3.4%)	38 (4.6%)
	NOSALLJ	174 (21.2%)	78 (9.5%)	21 (2.6%)
Tot		819 (100%)	221 (26.9%)	181 (22.1%)

events and to describe the environment associated with the MCSs.

SALLJ events were defined following criteria similar to those of Salio et al. (2002) and Nicolini and Saulo (2000), requiring that at least one of the four synoptic hours confirm the following:

- The flow must come from the north (originating in equatorial latitudes and reach subtropical latitudes) at low levels (850 or 925 hPa) with the wind speed greater than 12 m s^{-1} immediately east of the Andes close to Santa Cruz de la Sierra (17°S, 62°W);
- The meridional flow must be greater than the zonal flow in the entire region enclosed by the 12 m s^{-1} isotach;
- The wind speed must decrease by at least 6 m s^{-1} above the low-level maximum in the area enclosed by the 12 m s^{-1} isotach.

During the period studied in 2000–03, SALLJ events were diagnosed by GDAS in 35% of the days (Table 1). Seasonal variation of the frequency of SALLJ events is weak: 39% in spring, 36% in summer, and 30% in autumn. This is in agreement with Salio (2002), who found a spring maximum in a study covering 15 yr. The remaining days are called NOSALLJ events, which cover an extensive variety of synoptic situations, representing 65% of the three seasons studied.

3. Geographical distribution and characteristics of the MCSs

During the 3-yr period studied, 645 MCSs were detected satisfying the identification criteria specified in section 2. Over the seasons studied these systems are distributed as follows: 286 in summer, 202 in spring and 157 in autumn (Table 2). Systems that achieved their maximum extent north of 23°S were considered tropical, and the remainder were considered subtropical. Table 2 shows that subtropical systems represent 33.2% of the sample, and tropical systems represent 66.8%.

TABLE 2. Number of MCSs detected under SALLJ or NOSALLJ conditions, considering tropical or subtropical position.

Season	Day criteria	No. of MCSs		
		Tot	Tropical	Subtropical
Autumn	SALLJ	63 (9.8%)	28 (4.3%)	35 (5.4%)
	NOSALLJ	94 (14.6%)	57 (8.8%)	37 (5.8%)
Spring	SALLJ	112 (17.3%)	55 (8.5%)	57 (8.8%)
	NOSALLJ	90 (14.0%)	76 (11.8%)	14 (2.2%)
Summer	SALLJ	124 (19.2%)	76 (11.8%)	48 (7.4%)
	NOSALLJ	162 (25.1%)	139 (21.6%)	23 (3.6%)
Tot		645 (100%)	431 (66.8%)	214 (33.2%)

Figure 2 allows an analysis of seasonal and diurnal variations in the number and geographical location of tropical and subtropical MCSs, under SALLJ or NOSALLJ conditions. For the tropical area, the higher occurrence of MCSs is evident during summer, whereas in autumn MCSs in this region diminish in frequency and increase again in spring. This evidence highlights the tropical cycle of convection associated with the advance and retreat of the intertropical convergence zone. These systems basically attain their maximum development during the daytime, showing their highest frequency during the NOSALLJ days throughout the three seasons (Table 2).

As for the observed subtropical MCSs, they develop with greater frequency during SALLJ events in spring and summer (80.6% and 67%, respectively; Table 2); whereas in autumn MCSs do not show a clear correlation with SALLJ (48%). Subtropical MCSs show a preference for a nocturnal phase at a mature stage over Argentina, which contrasts with a daytime tendency over Uruguay and southern Brazil.

It is worth emphasizing that the systems in the whole region, reached their maximum development east of 65°W. This is not to say that there is no convection west of this meridian, but that the systems that develop over the slope of the Andes tend to be either smaller over their whole life cycle, or their maximum extent is attained after passing eastward of 65°W.

Histograms of hourly frequency of initiation, maximum extent, and decay are displayed in Fig. 3 in order to ascertain the times of genesis and evolution of MCSs. Two additional histograms for the size of the systems at maximum extent (Fig. 4) and for their total lifetime (Fig. 5) are included. As the breakdown for individual seasons reveals similar results, the following analysis comprises all three seasons and only highlights differences between seasons when they are significant.

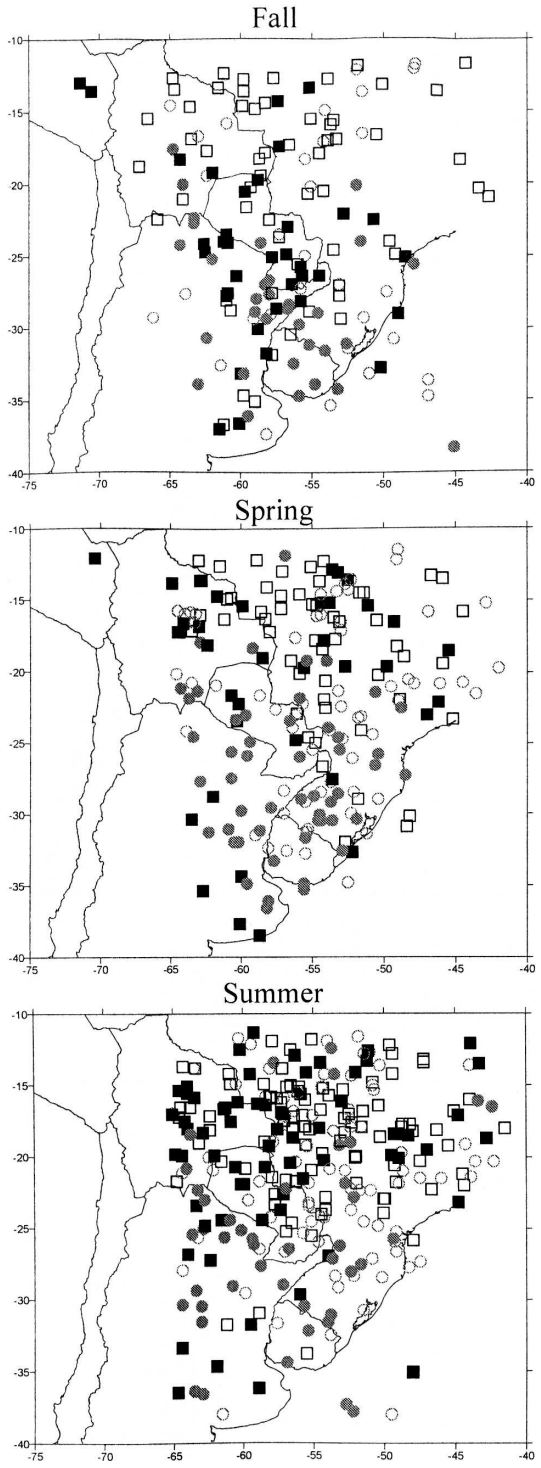

FIG. 2. MCS centroids at the time of maximum extent during (top) autumn, (middle) spring, and (bottom) summer. The MCSs indicated with a circle correspond to the systems that occurred during a day of SALLJ, whereas the squares indicate a NOSALLJ day. The open symbols indicate the systems that reached maximum extent during the day (between 1230 and 0000 UTC) while the full symbols show the systems that attained maximum extent at night (between 0030 and 1200 UTC).

As shown in Fig. 3, the tropical systems studied evolve in three overlapping periods of time. They tend to initiate between 1500 and 2100 UTC, which implies an association with the time of maximum radiative heating. As the day advances these systems tend to reach their maximum extent between 1800 and 0000 UTC, dissipating over the next 6 h (2100–0300 UTC). The systems that reach their maximum extent during the afternoon represent 62% of the sample, while the remaining 38% are predominantly scattered over the remainder 24 h. There are few systems that dominate during nighttime over the tropical area, and most are associated with squall lines. These nocturnal squall lines tend to originate over the coast of Brazil as an effect of convergence generated by the sea breeze during the afternoon or by low-level jet currents from the east, and then propagate inland at night, as Cohen et al. (1995) described for systems in equatorial Brazil. Tropical MCSs show a life cycle duration (Fig. 4) shorter than 9 h in 89% of the cases. This short lifetime suggests that they are mainly tied to the radiative heating cycle. Another important characteristic shown by tropical MCSs is their size at the time of maximum extent (Fig. 5), which in 65% of the cases is smaller than 150 000 km^2.

Subtropical systems show a maximum frequency of initiation between 1800 and 0000 UTC, which extends toward the nocturnal hours with a minimum before noon (Fig. 3). The maximum extent occurs over a wide range of hours; 60% are nocturnal, although no single strong peak dominates the sample. It is interesting that the minimum is observed near local noon (1500–1700 UTC) in both tropical and subtropical systems. Dissipation can take place at any time of the day. Subtropical MCSs, compared with tropical MCSs, attain a longer duration and a wider size range with an extreme value of 1.2×10^6 km^2. In SALLJ events, subtropical MCSs have a broad distribution of their life cycle stages, implying that the forcing from the low-level jet is more important than that from the diurnal cycle of heating, in contrast to tropical MCSs.

In the sample corresponding to years 2000–03, studied in the current paper, at least one large subtropical MCS developed in 41% of the SALLJ events in all seasons. In contrast, during NOSALLJ events this percentage dropped to 12% (Table 1). This result shows the importance of the synoptic conditions supplied by the SALLJ in the development of large subtropical MCSs.

MCSs are effective in causing precipitation over all the continents. In South America especially, MCSs explain 40% of the total continental precipitation using the Tropical Rainfall Measuring Mission (TRMM) observations (Nesbitt et al. 2000; Mota 2003). Over SESA

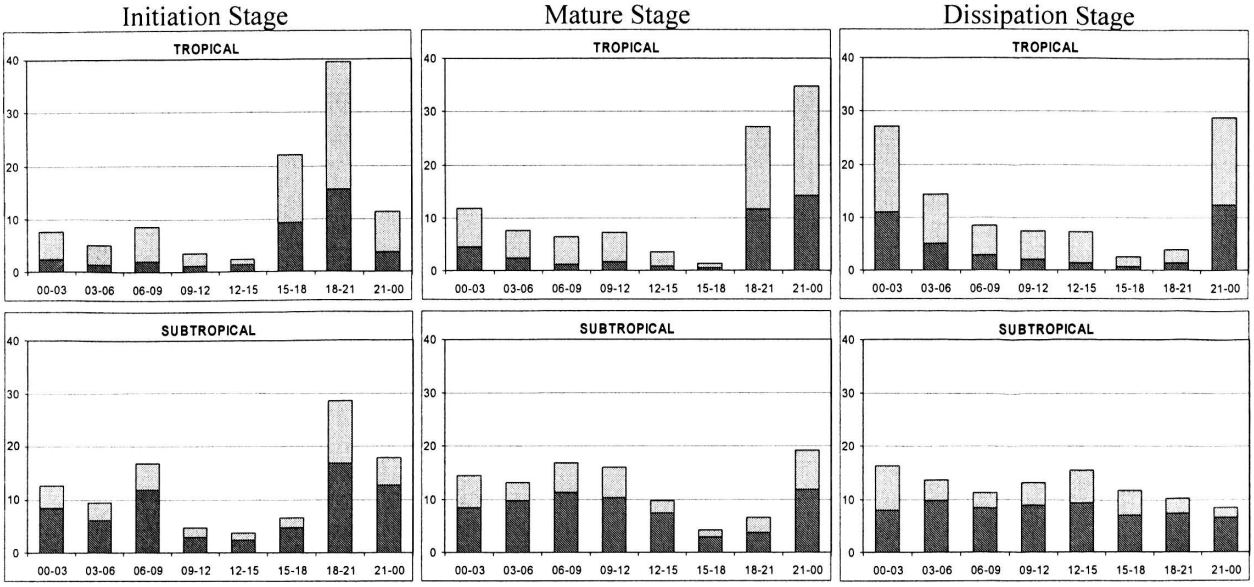

FIG. 3. Frequency distributions in percent of MCSs for SALLJ (dark gray) and NOSALLJ (light gray) samples of (left) initiation, (middle) maximum extent, and (right) dissipation time in UTC.

in particular, they contribute as much as 80% of the total precipitation (S. W. Nesbitt 2006, personal communication) and are dominant in the precipitation totals over the Plata basin. In addition, they generate emergencies and severe weather such as those documented by Silva Dias (1999). Given the high frequency of occurrence of MCSs mostly during the SALLJ events it is of interest to focus on the subtropical MCS–SALLJ sample to investigate the evolution of the synoptic patterns from the day prior to the MCS occurrence to the day after its occurrence.

A description of a 3-day evolution (centered on a MCS–SALLJ day) of the maps that depict the horizontal distribution of convection frequency is addressed in the following section. The objective is to recognize the extent and location of the areas where these systems more frequently occur over SESA and diurnal variability in these patterns. This description complements the overall diurnal life cycle and the geographical distribution of the position of the centroids at maturity, which have already been described.

4. Evolution of the geographical distribution of the frequency of convection

Convection frequency represented by an IR brightness temperature below 218 K was calculated over the whole domain (Fig. 1) and the evolution of its geographical distribution is displayed in Fig. 6 during the 3-day period centered on the MCS–SALLJ day. *This day is defined as one during which at least one selected MCS reaches its mature stage and also when the SALLJ criteria are verified*. Day −1 corresponds to the chronological day before, and day +1 corresponds to the day after. The MCS–SALLJ sample consisted of 117 days during the 2000–03 season. If a MCS also occurred on day −1 or day +1, this day was excluded from the sample in order to characterize patterns solely associated with the mesosystem cycle.

In tropical latitudes the convection frequency during this 3-day evolution shows a diurnal cycle characterized by a nocturnal maximum close to Santa Cruz de la Sierra, Bolivia, on the east slope of the Andes, and a typical radiative diurnal cycle is evident over Brazil and the lowlands of Bolivia.

As for the SESA region, the presence of a zone centered at 36°S, 60°W with a weak convection frequency involving an area of 400 000 km^2 was noted on day −1 at 0000 UTC (Fig. 6a). This maximum intensifies and spreads during the next 12 h (Figs. 6b,c), covering Uruguay and the entire center of Argentina, with an apparent decline at 1800 UTC (Fig. 6d). The contrast between figures at 1800 UTC corresponding to day −1 and the 0000 UTC corresponding to the MCS–SALLJ day is significant (Fig. 6e). A number of developments, not present in day −1, occur over the entire slope of the Andes and all over SESA. The frequency of convection intensifies at 0600 UTC and the concentration of its maximum at 1200 UTC is the main difference with respect to 6 h before (Figs. 6f,g). The absolute maximum

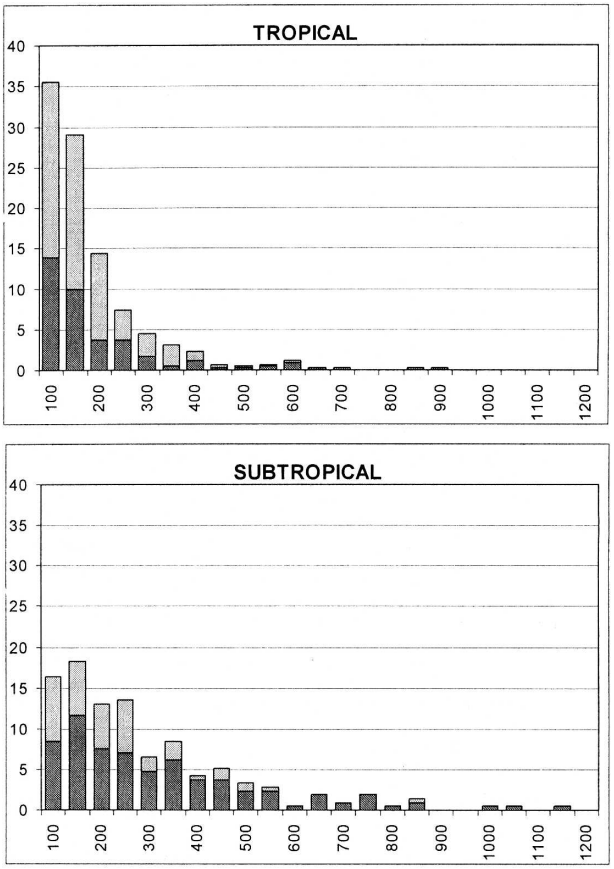

FIG. 4. Frequency distributions in percent of MCSs for SALLJ (dark gray) and NOSALLJ (light gray) samples of size at maximum extent time in 10^3 km^2.

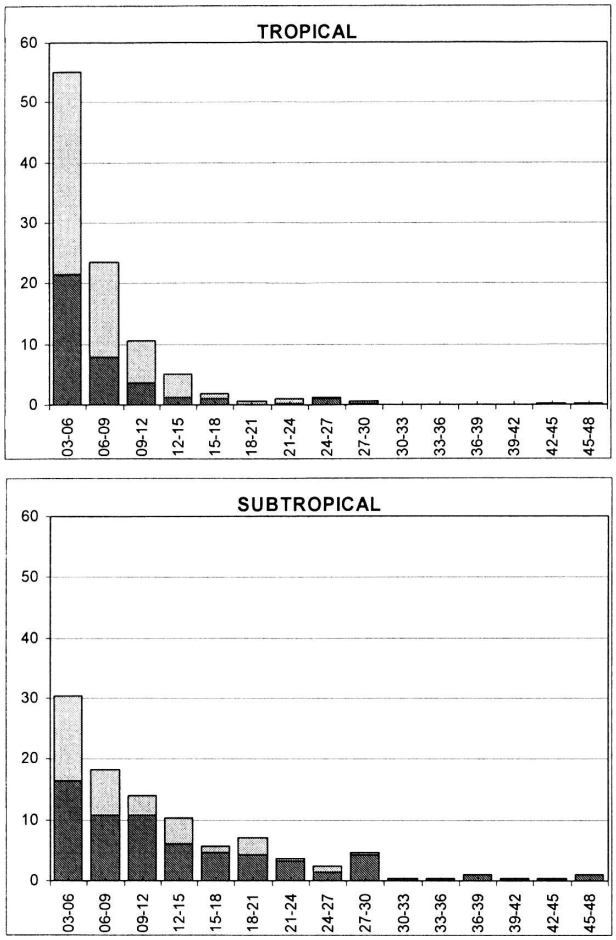

FIG. 5. Frequency distributions in percent of MCSs for SALLJ (dark gray) and NOSALLJ (light gray) samples of duration of the life cycle in hours.

occurs at 1030 UTC attaining a value of 35% at 29°S, 58°W. This nocturnal extreme subsides toward the afternoon (1800 UTC), showing a displacement north of 25°S and toward Uruguay (Fig. 6h).

On day +1 there is a clear weakening of the systems in subtropical areas and an intensification in tropical latitudes (Figs. 6i–l). While at 0000 UTC, the pattern shows two distinct bands, one with a northwest–southeast orientation over the Argentine–Paraguayan frontier and the other to the south centered on 31°S, 63°W; the configuration at 1800 UTC shows a northward displacement of the systems to north of 24°S.

5. Environment associated with subtropical MCSs during SALLJ events

The mean GDAS fields were calculated for the MCS–SALLJ day, day −1, and day +1 for the purpose of describing the environment in the synoptic and meso-alpha scales associated with the MCS–SALLJ day and its temporal evolution. This compositing technique was applied over the available 6-h GDAS operational fields.

a. Vertically integrated moisture flux

The vertically integrated moisture flux **Q** and its divergence were calculated by the method applied by Salio et al. (2002). These fields are illustrated at 12-h intervals in Figs. 7 and 8, respectively. On day −1 a continuous moisture flux from the north is evident at 0000 UTC, which penetrates meridionally into extratropical latitudes up to 30°S (Fig. 7a). At 1200 UTC the flux shows an intensity that surpasses 500 kg m^{-1} s^{-1} south of Santa Cruz de la Sierra (Fig. 7b). This value is higher by 20% than the one determined by Salio et al. (2002) for strong SALLJ events that reach subtropical latitudes during summer. This mean moisture flux pattern mirrors the characteristics of the particular SALLJ event that extends southward (Salio et al. 2002; Nicolini

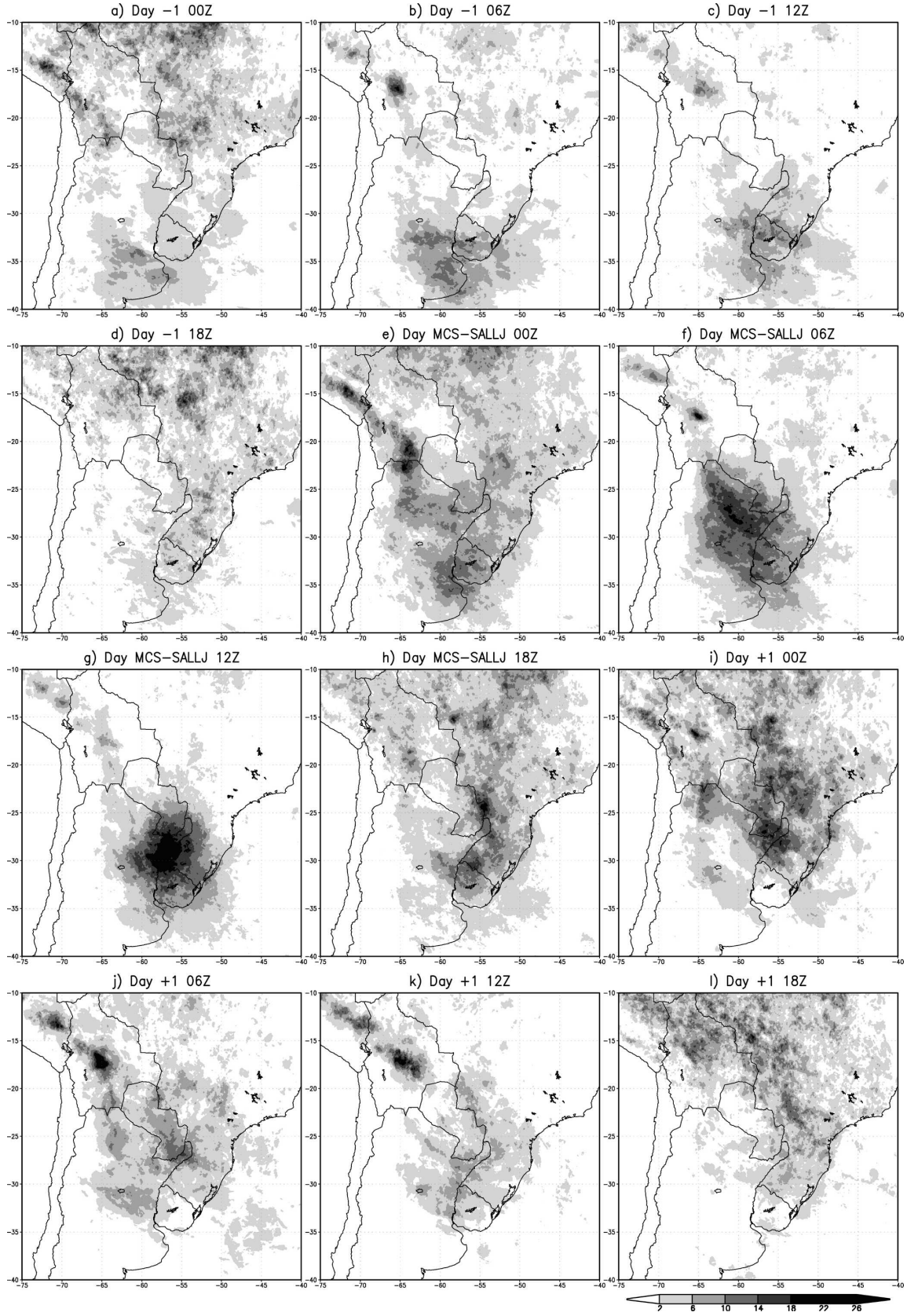

FIG. 6. Geographical distribution of the frequency of convection represented by an IR brightness temperature below 218 K. Frequencies are shown for the MCS–SALLJ day, the day before (day −1), and the day following (day +1) every 6 h.

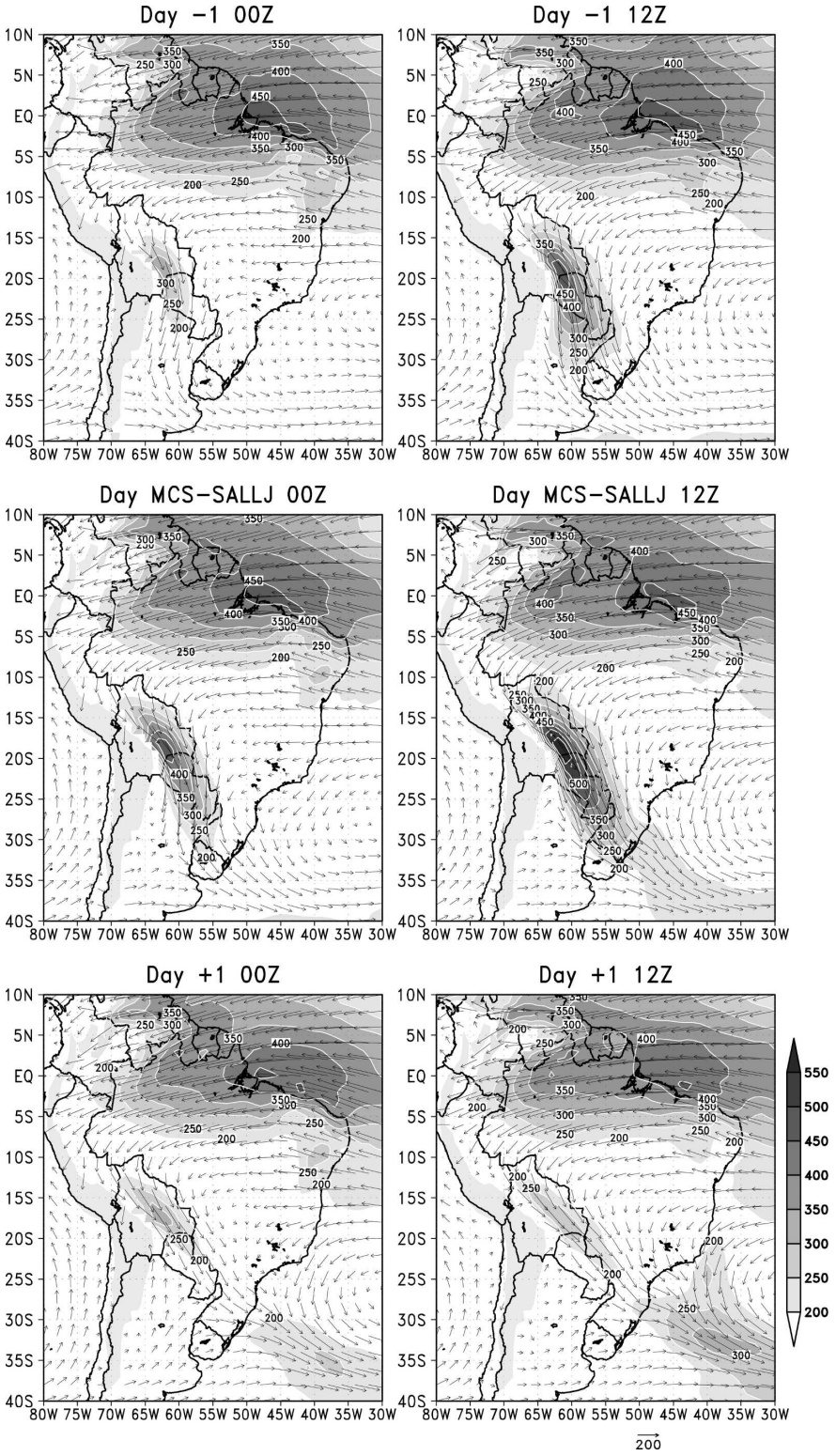

FIG. 7. Vertically integrated moisture flux (vectors) and its absolute value (shaded) in kg m^{-1} s^{-1} for the MCS–SALLJ day, the day before (day −1), and the day following (day +1) every 12 h. Values greater than 100 kg m^{-1} s^{-1} are shaded. No calculations are made for mountain areas higher than 1500 m (dark shading).

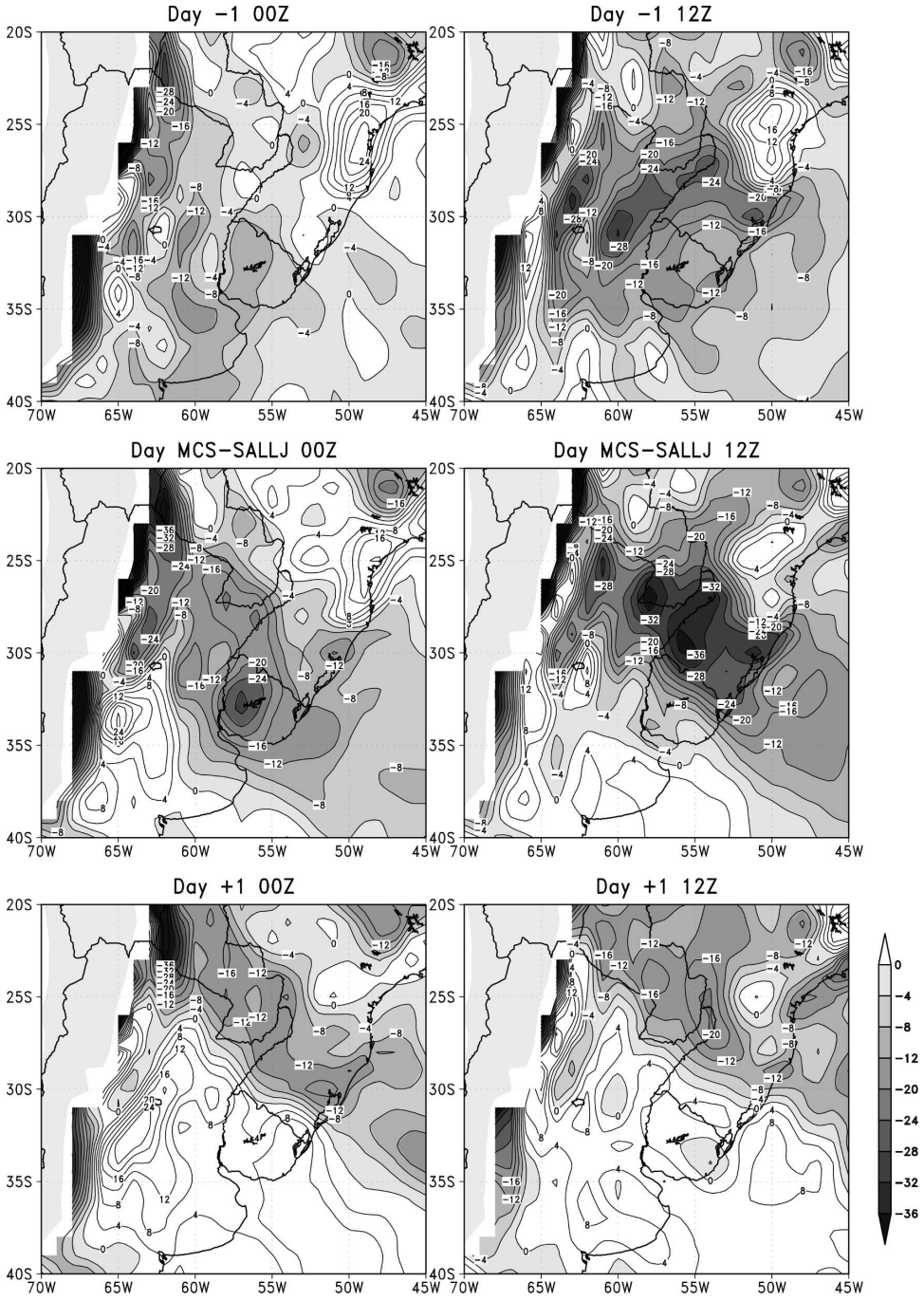

FIG. 8. Divergence of the vertically integrated moisture flux in 10^{-5} kg m^{-2} s^{-1} (convergence areas are shaded) for the MCS–SALLJ day, the day before (day −1), and the day following (day +1) every 12 h. No calculations are made for mountain areas higher than 1500 m.

and Saulo 2006) at 1200 UTC in the 850-hPa wind field. This is dominated by an extensive low-level jet that reaches 25°S, east of the Andes (figure not shown), generating an important transfer of moisture over northern and central Argentina on day −1.

The entire SESA region is under the influence of the deceleration of the moisture flux and, therefore, of the associated convergence on day −1 at 0000 UTC (Fig. 8a). This field depicts a strong **Q** convergence over the eastern slope of the Andes and a maximum located at 35°S, 61°W. At 1200 UTC convergence intensifies in this secondary maximum in accordance with the in-

crease of the magnitude of the flux toward the south and the development of a few systems over central Argentina and Uruguay (Fig. 8b).

At 0000 UTC on the MCS–SALLJ day, the frequency of convection showed that MCSs are in their initial phase and extend all over central Argentina. The mean centroid of their initiation stage is located at 29°S, 59°W (Fig. 6e). The **Q**-divergence field presents a convergence zone around the above position (Fig. 8c). Convection and moisture convergence are closely related, they basically coexist when convection is present but it is important to remark that systems are not yet developed at 1800 UTC of day −1 (Fig. 6d) in central Argentina. At this moment the **Q** field and its divergence display (figure not shown) a pattern equivalent to that shown at 0000 UTC of the MCS–SALLJ day, evidencing the presence of convergence before the development of the systems and the presence of one ingredient that helps trigger convection in the area. This behavior is opposed to the climatological mean SALLJ diurnal cycle, mostly forced by boundary layer mechanisms, which has a minimum at these hours (Marengo et al. 2004), indicating a synoptic-scale sustained contribution of moisture during the day prior to the occurrence of the system. Toward 1200 UTC of the MCS–SALLJ day the moisture flux starts to deviate eastward, showing peak values that exceed 550 kg m^{-1} s^{-1} (Fig. 7d). The **Q** convergence also reaches its maximum and predominates over northeast Argentina, southern Brazil, and Uruguay and overlaps with the maximum convection frequency (see Figs. 6 and 8d).

Toward 0000 UTC of day +1, the **Q** field shows a marked northwest–southeast orientation showing an exit area in southern Brazil, while central Argentina and Uruguay are influenced by southerlies and divergence of **Q** (Fig. 7e). This exit area is coincident with the one corresponding to an elongated maximum in the convection frequency field, shown in Fig. 6, at the same time. The presence of systems dominated by the divergence area in the area localized over central Argentina may be because, in 54% of the cases studied, day +1 is still a SALLJ event that penetrates beyond 25°S. For this reason, in some isolated cases convection still exists over northern Argentina, but the predominating pattern is characterized by a northward displacement of the systems.

Before proceeding, a natural question that arises is what is different about the 59% of the SALLJ days without large and long-lived subtropical MCSs. Marengo et al. (2004) and Salio et al. (2002) gave a partial answer in distinguishing SALLJ events that penetrated poleward of 25°S, which favored strong precipitation rates over SESA. The major feature of the SALLJ without subtropical MCSs is that the moisture flux in subtropical latitudes becomes more zonally oriented (toward the east) where it favors moisture convergence over eastern Brazil or along the South Atlantic convergence zone (Fig. 9a). Further insight into this difference between both SALLJ samples is gained by looking at Fig. 9b, which confirms a strong southerly moisture flux anomaly over northern and central Argentina on the day before to the occurrence of the MCS. Differences are not significant between both samples on the MCS–SALLJ day (Fig. 9c).

b. Synoptic pattern evolution

The representation of the evolution of the atmospheric fields in the synoptic scale is illustrated with the geopotential at 850 hPa, the 1000–500-hPa thickness, and streamlines at 200 hPa. Day −1 shows the presence of a deep and warm trough east of the Andes at 850 hPa, which extends from 35° up to 15°S (Figs. 10a and 11a). The warming and the deepening of the trough, apparent in a positive tendency in the thickness field and in a negative geopotential tendency, respectively, are coherent with an increase in the northerly flow, as previously displayed in the **Q** field. A conspicuous thermal contrast denotes the presence of an extensive baroclinic zone located between 30° and 37°S, east of the Andes. These low- and midlevel features are also present during poleward extended SALLJ events but they are more clearly depicted in the present composite. Particularly, the negative geopotential tendency shown in Fig. 10a has been associated with a deep low, located over northwestern Argentina during the extreme SALLJ events mentioned before (Nicolini and Saulo 2000; Salio et al. 2002; Saulo et al. 2004). At high levels, a deep trough is observed with its axis at 80°W on day −1 at midlatitudes (Fig. 12a). At this position there is a wind maximum at high levels centered at 36°S, 60°W, which corresponds to a jet streak related to the baroclinic zone.

On the MCS–SALLJ day, the baroclinic zone positioned south of Buenos Aires advances toward the northeast (Fig. 11b). All of central and southern Argentina are immersed in a negative 1000–500-hPa thickness tendency zone (Fig. 11b). Behind the trough, associated with the baroclinic zone, a strong positive geopotential tendency is observed (Fig. 10b). The low at 850 hPa weakens and shifts northward, similar to the findings of Nicolini et al. (2002). At high levels there is an eastward progress of the trough that, at this stage, is located over the Andes. The jet streak intensifies,

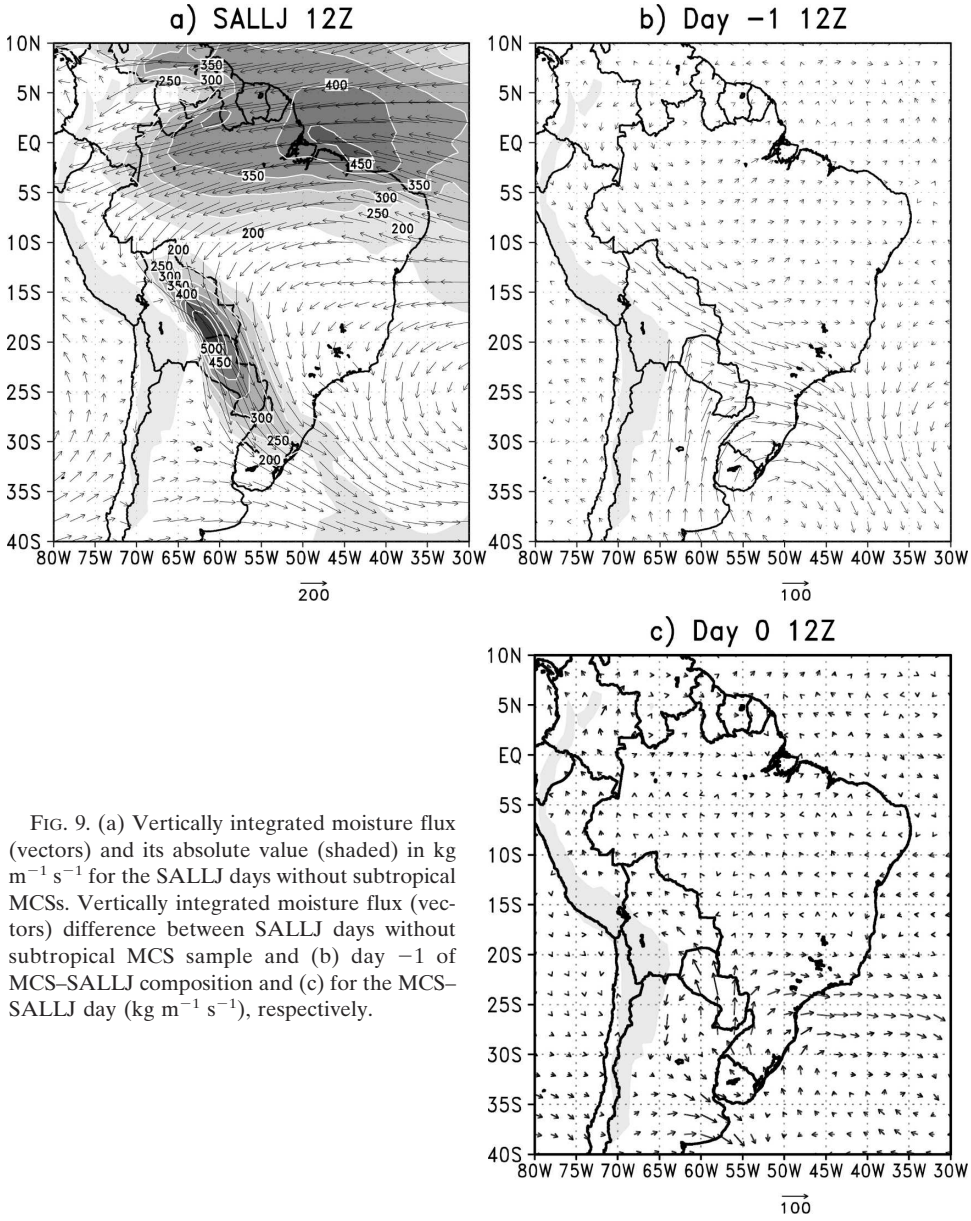

FIG. 9. (a) Vertically integrated moisture flux (vectors) and its absolute value (shaded) in kg m^{-1} s^{-1} for the SALLJ days without subtropical MCSs. Vertically integrated moisture flux (vectors) difference between SALLJ days without subtropical MCS sample and (b) day −1 of MCS–SALLJ composition and (c) for the MCS–SALLJ day (kg m^{-1} s^{-1}), respectively.

reaching an extreme of 45 m s^{-1} at 39°S, 50°W (Fig. 12b).

On day +1 the 1000–500-hPa thickness field in Fig. 11c shows a persistent northeastward displacement of the baroclinic zone and a marked reduction of the thickness over a northwest–southeast axis throughout central and northern Argentina and Uruguay, which extends over the Atlantic to 30°W. A strong extreme of positive geopotential tendencies is observed over northwestern Argentina at 850 hPa, while negative tendencies are displaced toward the Atlantic and southern Brazil (Fig. 10c). Finally, the 200-hPa fields show an eastward displacement of the jet streak and the progression of the negative geopotential tendencies toward the east and a zonal structure of the streamline field (Fig. 12c).

c. Dynamic and thermodynamic structure

At 1200 UTC of day −1 there is a wind maximum between 18° and 27°S centered at 850 hPa (Fig. 13b), which spreads with respect to the previous hour (Fig. 13a). This low-level wind maximum is immersed in a zone of high equivalent potential temperature θ_e with maximum surface values close to 345 K. The θ_e field shows convective unstable conditions up to 600 hPa north of 36°S, where a convectively neutral atmosphere

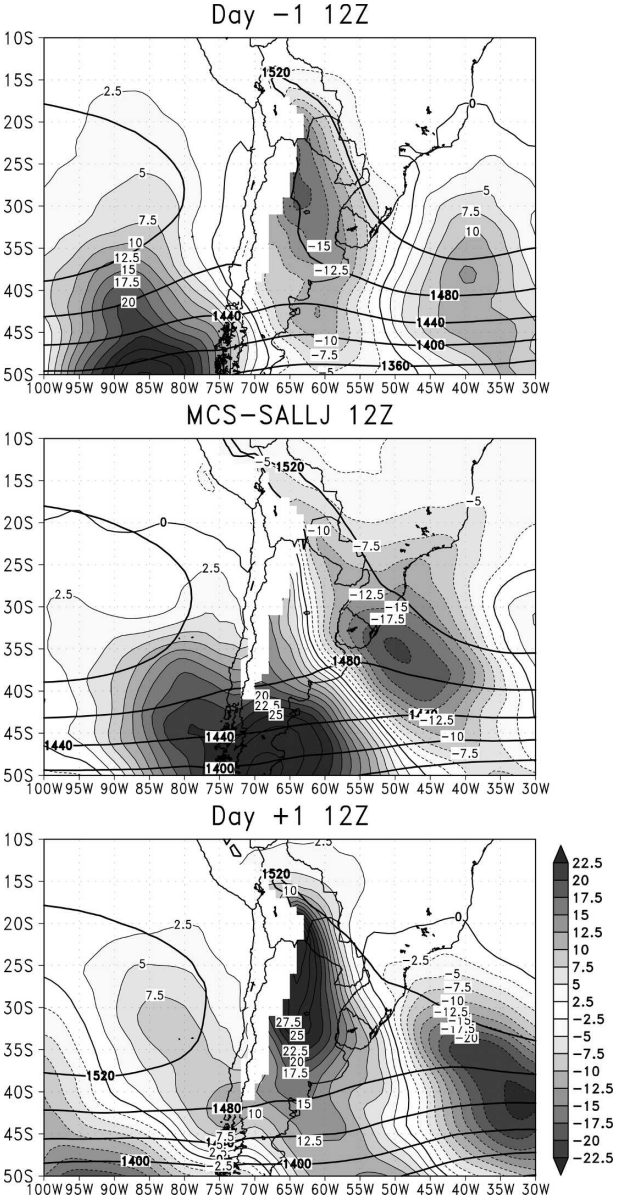

FIG. 10. Geopotential height (m, lines) and 24-h tendency (m every 24 h, shaded) at 850 hPa for the MCS–SALLJ day, the day before (day −1), and the day following (day +1) at 1200 UTC. No calculations are made for mountain areas higher than 1500 m.

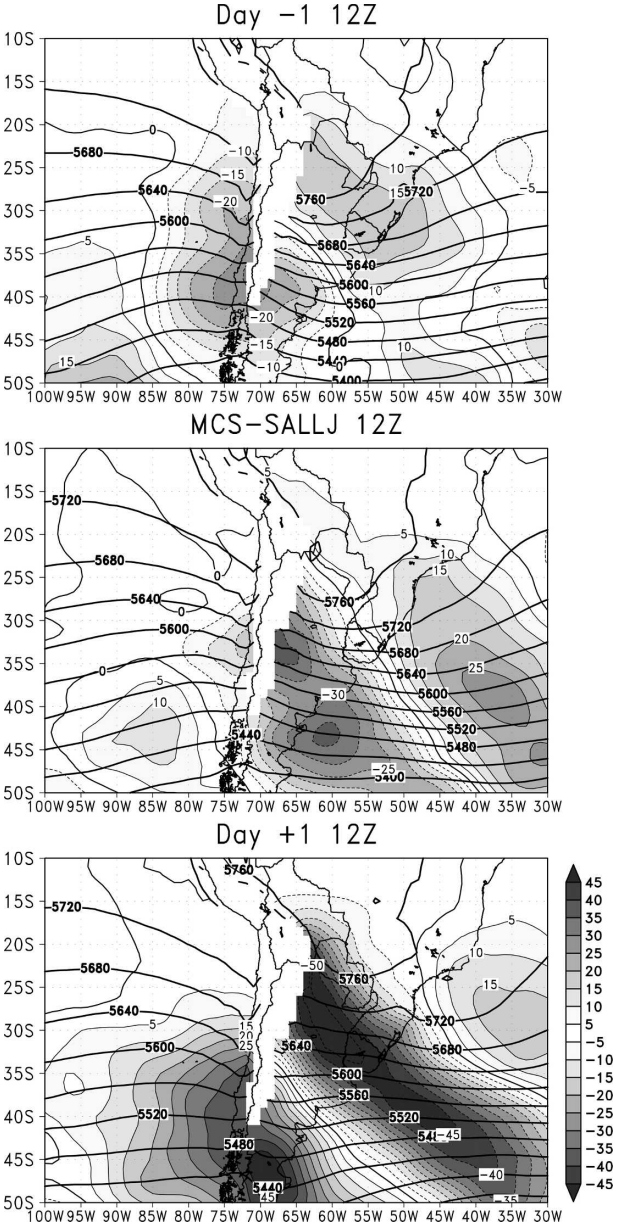

FIG. 11. Geopotential thickness between 1000 and 500 hPa (m, lines) and 24-h tendency (m every 24 h, shaded) for the MCS–SALLJ day, the day before (day −1), and the day following (day +1) at 1200 UTC. No calculations are made for mountain areas higher than 1500 m.

is observed. The wind maximum from the northwest at 200 hPa is centered at 36°S evidencing the leading side of the trough shown in Fig. 12a.

The maximum of the northerly flow rises to 750 hPa in the afternoon hours (1800 UTC; Fig. 13c) although the jet profile persists at this time. This behavior of the wind profile shows, once again, a marked difference with respect to the typical SALLJ profile at this time in subtropical latitudes described in previous literature. Particularly, the abscence of a jetlike profile at 1800 UTC has been documented using the experimental SALLJEX observations and similar analyses to those employed in this paper (Nicolini et al. 2002; Marengo et al. 2004; Nicolini et al. 2004). The atmosphere in the present composite analysis is convectively unstable with θ_e surface values higher than 350 K, a typical observed threshold value associated with MCS situations in this area.

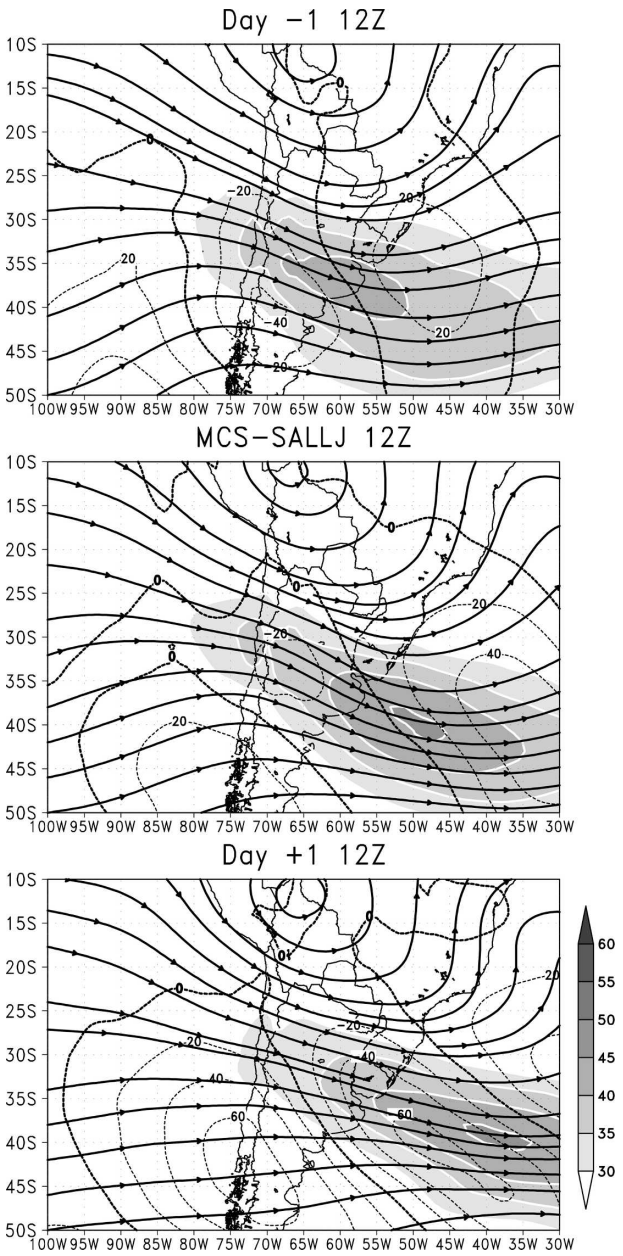

FIG. 12. Streamlines, 24-h geopotential tendency (m every 24 h, labeled contours), and wind velocity higher than 30 m s^{-1} (shaded, scale below) at 200 hPa for the MCS–SALLJ day, the day before (day −1), and the day following (day +1) at 1200 UTC.

At the time when there is a maximum in genesis of systems north of 36°S (0000 UTC of the MCS–SALLJ day; Fig. 13d), there is a strong increase (5°C) in the θ_e over the core and downstream of the low-level jet, associated with the entry of a tongue of warm and humid air in a convectively unstable atmosphere. During the MCS–SALLJ day, the low-level jet profile of the northerly flow is evident at all hours, reaching the highest values at 0600 and 1200 UTC (Figs. 13e,f), which surpass 12 m s^{-1} at 23°S. The θ_e field reaches a maximum at 0600 UTC immediately north of the concentrated area of convection frequency (Fig. 6g). The northerly flow starts to retreat at 1200 UTC and this behavior is more clearly manifest at 0000 UTC of day +1 when the flow is confined north of 23°S and the low-level jet profile disappears. A marked decrease in the θ_e values and convective instability are observed between 0000 UTC of the MCS–SALLJ day and 0000 UTC of day +1, exhibiting a less favorable environment for convection south of 25°S. These previous results show the presence of the low-level jet before the genesis of the MCSs and upstream of their future position, showing its triggering role in the development of the MCSs. But once convective systems attain their maximum frequency of development, the low-level jet reaches its greatest intensity, suggesting the possible role of the latent heat release in the acceleration of the wind and a possible feedback between the low-level jet and the precipitation at its exit region (Nicolini et al. 1993).

Focusing on the significant hours, Fig. 14 shows vertical cross sections of the horizontal advection of temperature and specific humidity. The magnitude of the specific humidity advection denotes the important role of the low-level jet in the humidity transport into subtropical regions before the development of the MCSs (Figs. 14a,b). The moisture availability is at a maximum at 1800 UTC of day −1, between 25° and 35°S, and persists over the whole life of the systems. Extreme values of specific humidity (16 g kg^{-1}) are attained close to the surface and before the development of the systems. Specific humidity increases up to 18 g kg^{-1} north of 25°S at the dissipation time (figure not shown). These values are extremely high for individual situations, showing again the extreme conditions that dominate during the whole organized convection life cycle. The dissipation of the systems is in phase with the decay of the low-level jet and its related moisture transport, and therefore with its reduced efficiency in feeding downstream convection (Figs. 14e,f). Likewise, the positive horizontal advection of temperature plays an important role in warming low levels from 1800 UTC of day −1 to 1200 UTC of the MCS–SALLJ day and reaches its extreme value when the low-level jet is maximum (Fig. 14c).

The presence of the low-level jet and of the equatorward side of a jet streak at high levels lead to a classical pattern of convergence and ascending motion shown in Fig. 15. Especially at 1800 UTC of day −1, convergence at low levels is depicted in subtropical areas, downstream of the low-level jet position (Fig. 15a), whereas divergence maximizes at 200 hPa. At this hour the pat-

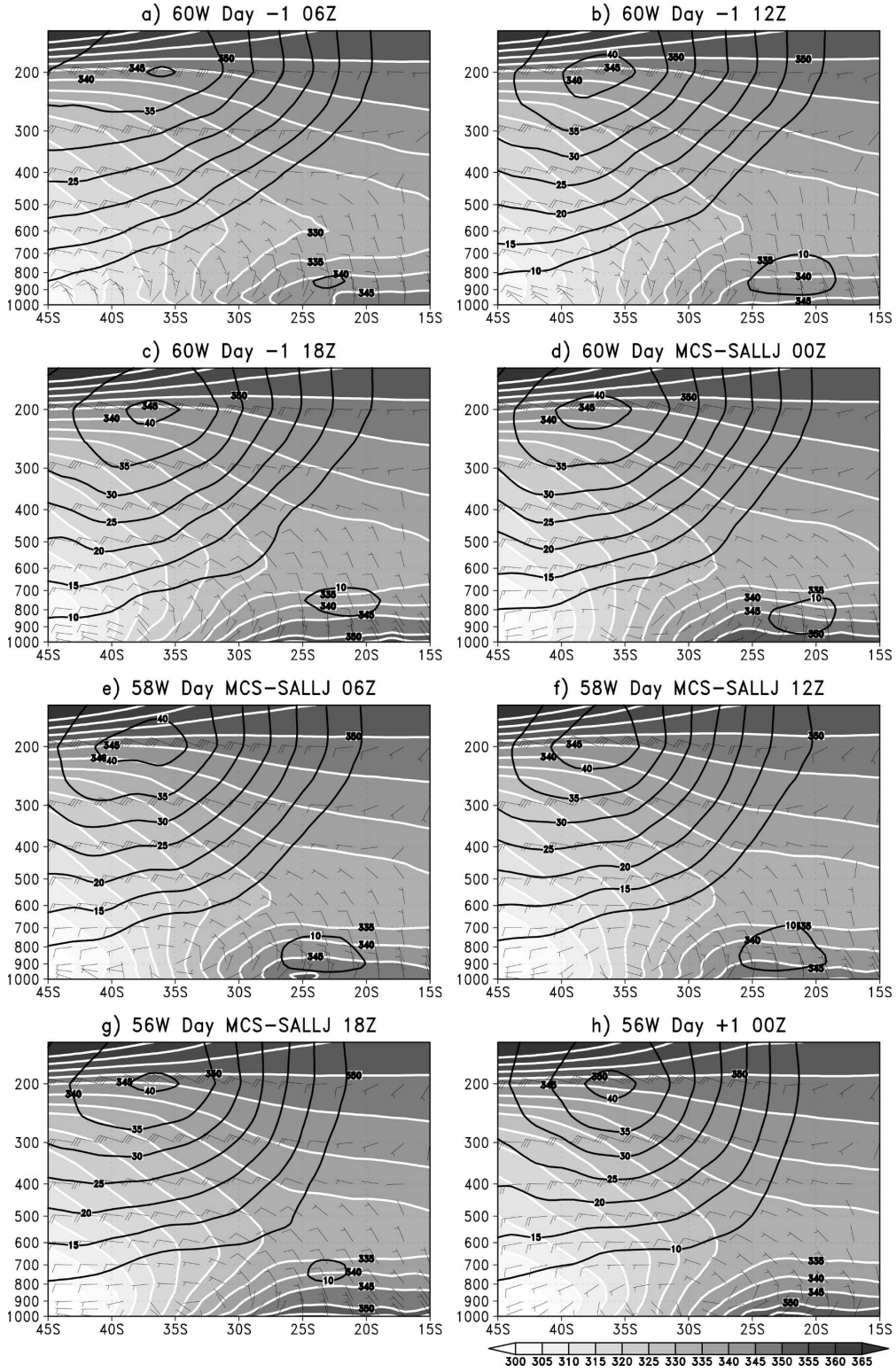

FIG. 13. Vertical cross sections of θ_e (K, thin contours with shading), wind barbs, and wind speed (thick contours). Reference vector for the wind of 30 m s^{-1} is indicated at the bottom. All panels cover a latitudinal range from 45° to 15°S and are 6 h apart. The longitudes shift slightly eastward with time during the MCS–SALLJ day, following the axis of the low-level jet as it shifts eastward.

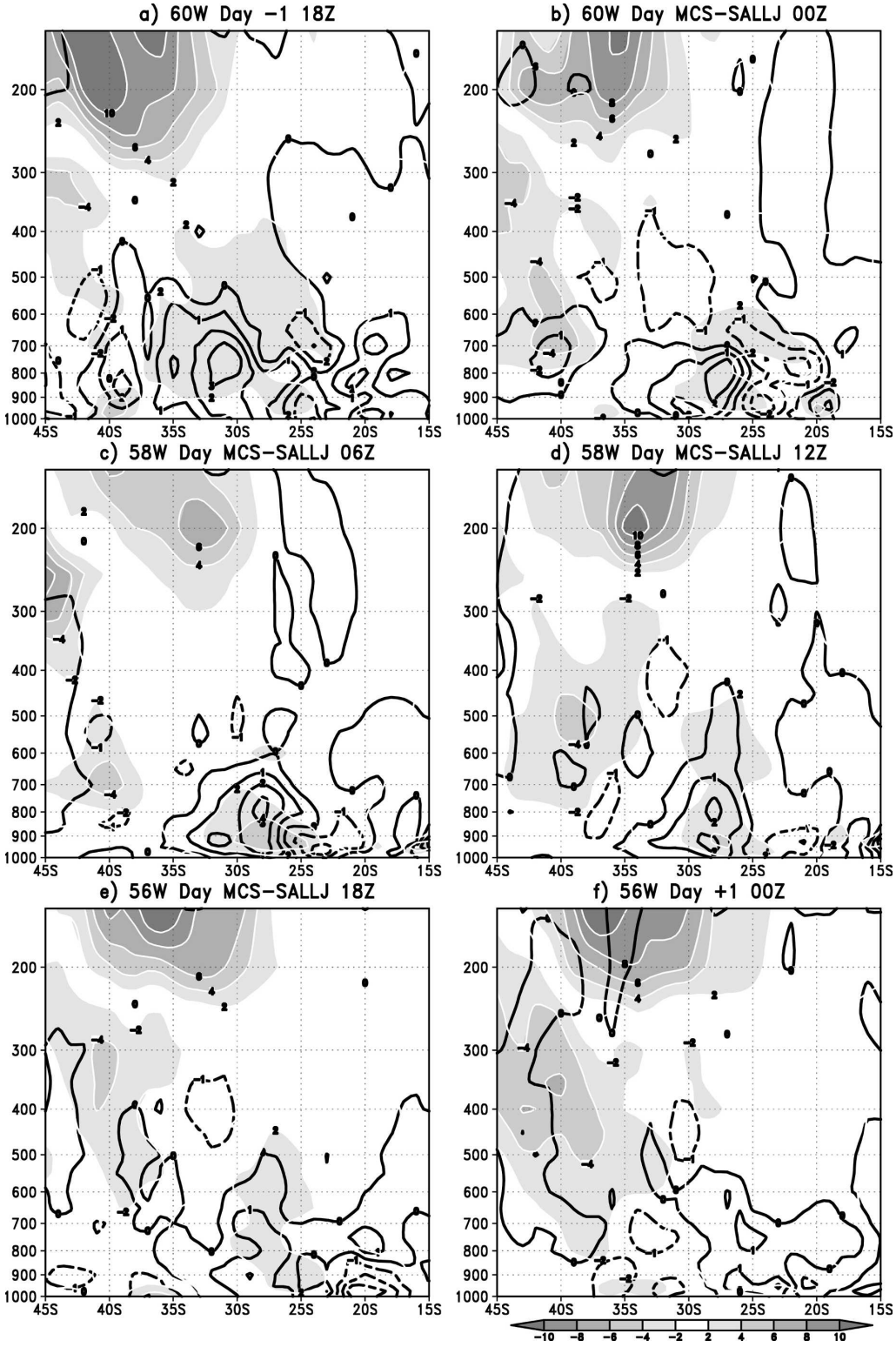

FIG. 14. Vertical cross sections of the horizontal advection of specific humidity (g kg^{-1}) every 24 h (lines) and horizontal advection of temperature tendency (degrees) every 24 h (shaded, scale below). All panels cover a latitudinal range from 45° to 15°S and are 6 h apart. The longitudes shift slightly eastward with time during the MCS–SALLJ day, following the axis of the low-level jet as it shifts eastward.

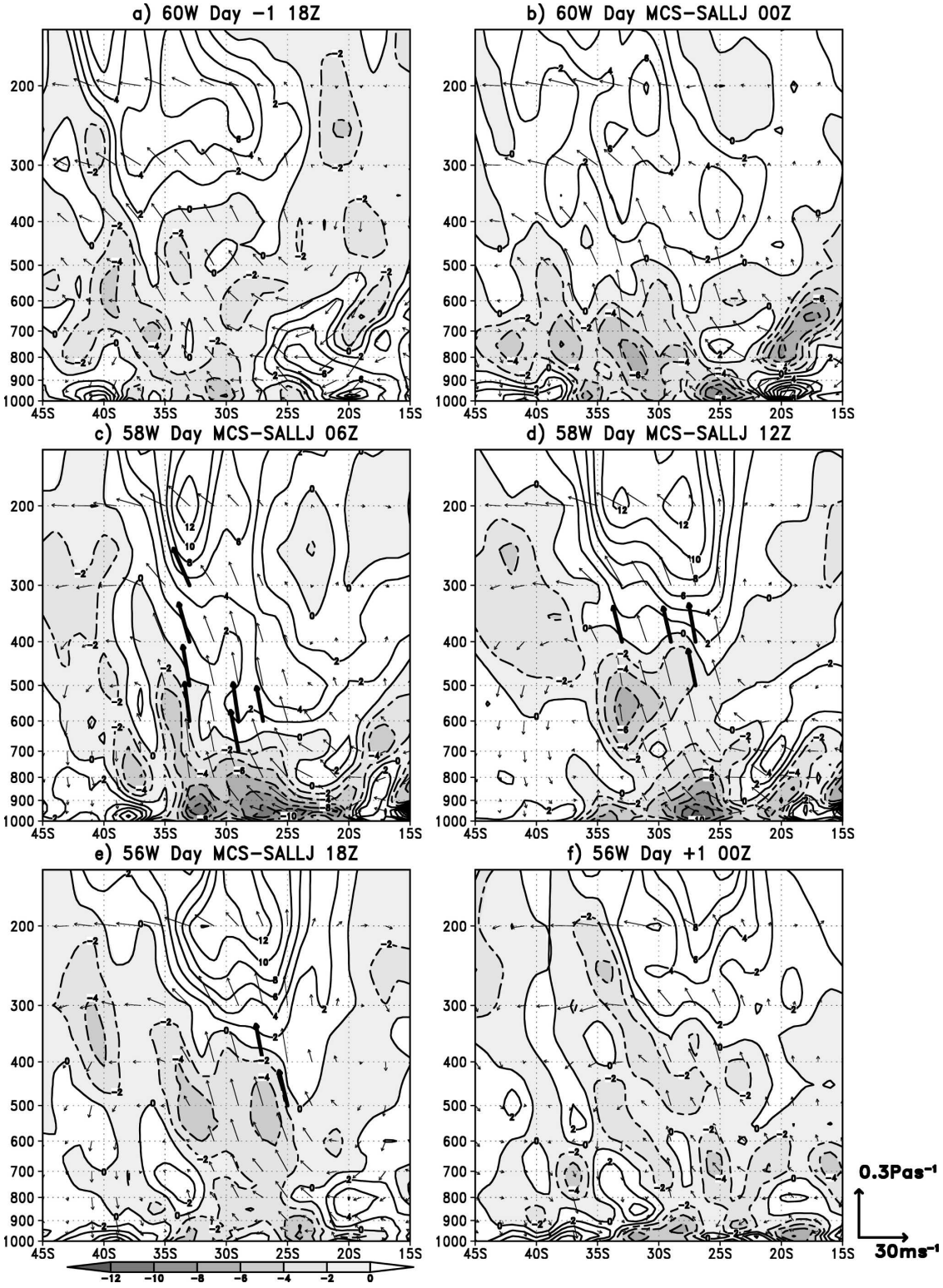

FIG. 15. Vertical cross sections of the meridional circulation (v, ω) and wind divergence (10^{-6} s^{-1}, thin lines). Convergence areas are shaded, scale below. Reference vector of the circulation is indicated at the bottom, 30 m s^{-1} in the horizontal and 0.3 Pa s^{-1} in the vertical. Vectors, where the vertical velocity is higher than 0.2 Pa s^{-1}, are thicker. All panels cover a latitudinal range from 45° to 15°S and are 6 h apart. The longitudes shift slightly eastward with time during the MCS–SALLJ day, following the axis of the low-level jet as it shifts eastward.

terns of convergence and divergence are not disturbed by the presence of large MCSs because this is a time of minimal frequency of convection at these latitudes (Fig. 6d). Vertical motions are not observed in the maximum wind area at 750 hPa whereas ahead of its core there are weak rising vertical motions that attain 1.5×10^{-1} Pa s^{-1} at 36°S and 500 hPa, close to the nondivergence level. The vertical velocity values are of the same order as those found by Nicolini et al. (2002) and Cotton et al. (1989) for the initiation phase of MCSs.

At 0000 UTC at 60°W maximum convergence downstream of the low-level jet close to the surface reaches a value one order of magnitude higher than 6 h before (-1.0×10^{-5} s^{-1}). On the other hand, the high-level divergence and low-level convergence structure, provided by the entrance of the jet at 200 hPa, is preserved. The intensity of the vertical ascending motions at 33°S increases and extends in the vertical consistent with the increase of the low-level convergence and also with the beginning of organized deep convection (Fig. 15b). This pattern persists during the next 12 h (Figs. 15c,d), but now, the development of convection performs an acceleration of the low-level jet and an intensification of this pattern characterized by convergence at low- and midlevels combined with divergence at high levels. As the systems move to the northeast and start to reduce their frequency, surface convergence significantly diminishes at 56°W (1800 UTC of the MCS–SALLJ day; Fig. 15e), while convergence at midlevels and divergence at high levels continue with a similar intensity. This decline in the surface convergence is related to a deviation of the axis direction of the low-level jet resulting from a northward baroclinic zone displacement. At 0000 UTC of day +1 (Fig. 15f) the high-level divergence and rising motions decline over the area south of 25°S, accompanying the decay of the subtropical convection.

6. Summary

Tropical MCSs are smaller in size with respect to subtropical ones, and their lifetimes are only 6–9 h, with their initiation occurring mainly in the afternoon and dissipation in the early morning hours in accordance with the radiative cycle.

Subtropical MCSs develop with greater frequency during SALLJ events during the warm season, whereas in autumn the existence of a relationship between MCSs and SALLJ is not so evident. Subtropical MCSs have a greater initiation frequency between 1800 and 0000 UTC and later on, during maturity a marked nocturnal character over Argentina tends to show a greater frequency of events. During the daytime, convection tends to shift into Uruguay and southern Brazil. While tropical systems possess strong seasonal variability associated with the displacement of the intertropical convergence zone, subtropical systems show lesser variability as a function of season.

Subtropical MCSs, in contrast with tropical systems, frequently acquire extreme spatial and temporal extent, especially during SALLJ days. The detection of subtropical MCSs during the 2000–03 period demonstrates the high frequency of occurrence of this type of organized convection (41%) found during the SALLJ days, whereas on NOSALLJ days this frequency is only 12%. This result shows the importance of the synoptic conditions provided by the SALLJ for the development of MCSs and motivates the study of the atmospheric large-scale structure that evolves in close coexistence between SALLJ and subtropical organized convection at the mature stage.

The convection frequency for the MCS–SALLJ day, and the previous and subsequent days, shows the existence of systems south of 33°S during the early morning and dawn hours of day −1 (0000–1200 UTC). In the afternoon of day −1 (1800 UTC) those systems dissipate only to show an important development extending all over northern Argentina just before 0000 UTC of the MCS–SALLJ day. The absolute convection frequency maximum during the MCS–SALLJ day centered over northeast Argentina is nocturnal and subsides toward the afternoon, showing a northward displacement up to 25°S and eastward toward Uruguay at 1800 UTC of the MCS–SALLJ day. On day +1 there is a clear weakening of the subtropical systems, but intensification in tropical areas.

This increased frequency of convection over northeast Argentina is preceded by an intense transport of heat and moisture at low levels, which penetrates extensively into the subtropical areas on day −1. This flux presents a vertical low-level jet profile with an anomalous diurnal cycle denoted by a persistence of strong low-level winds during afternoon hours and generates convective instability, consequently enabling a gradual building of optimal conditions for the formation of the largest organized convection in the subtropical area during the following day. An additional contribution to the formation of convection is manifested by the favorable large-scale conditions given by the presence of a baroclinic zone at 36°S, which helps sustain ascending vertical motions in the area of MCS development. At 0600 and 1200 UTC of the MCS–SALLJ day the low-level heat and moisture contribution, the high-level divergence associated with the jet streak, the low-level convergence generated by the low-level jet, and the maximum regional values for surface specific humidity

and θ_e get into phase to create an extensive area with formation and intensification of organized convection. These processes have been previously identified by other authors as being responsible for the gradual destabilization of the atmosphere and the buildup of the required conditions to generate organized convection in other geographical regions (Johnson and Mapes 2001; Fritsch and Forbes 2001 and references therein).

The northeastward displacement and later dissipation of convection at 1800 UTC of the MCS–SALLJ day are markedly affected by a northward advance of the baroclinic zone, by a related cold advection in low levels and by a divergence of moisture flux contributing to the stabilization of the atmosphere. These processes inhibit subtropical convection and enable the possibility for systems to develop in tropical areas.

These results demonstrate the coevolution and interrelationship of SALLJ and long-lived subtropical MCSs. Such events are characterized by a southward penetration of the northerly low-level flow up to 35°S on the day prior to the development of the MCS. In terms of precipitation, Nicolini and Saulo (2006), using short-range regional weather forecasts and compositing the 1997–98 warm season SALLJ events also penetrating into subtropical latitudes, also found that these events are characterized by intense precipitation over SESA. The present paper reinforces their model results on the diurnal cycle of precipitation, nocturnal over Uruguay and the central part of northern Argentina, and diurnal over northwestern Argentina and southeastern Brazil. On the other hand, there are some differences when considering the two consecutive days (−1 and MCS–SALLJ). On day −1, most of the convective developments over SESA are observed to occur during the afternoon and evening, while on the second day the signal is clearly nocturnal (related to the maturing of the convection initiated the previous day). The earlier phase in maximum precipitation cannot be identified in Nicolini and Saulo (2006), because their compositing methodology averages consecutive days that, according to the present work, have different diurnal cycles. The agreement is good on the MCS–SALLJ day, emphasizing the dominance of the nocturnal phase that defines this particular day in contrast with the one that characterizes day −1. All these elements show the necessity of a persistent northerly flux extending far southward during at least one full day in order to build the optimal conditions for long-lived MCSs to develop.

A number of questions remain to be answered regarding the interaction between the SALLJ and MCSs. This paper focuses on the study of this relationship from a synoptic point of view, but there is a strong mesoscale component related to the presence of the Andes. Mountains control the development, maintenance, and decay of both systems, and it is still unknown how their interaction evolves. The SALLJEX experiment enhanced observations in the data-sparse region during the austral warm season 2002–03. This observational dataset together with high-performance mesoscale numerical models may be useful in future studies to address some of these topics.

Acknowledgments. This research is supported by UBA Grant X266 and TX30, ANPCyT Grant PICT 07-14420 and 07-06671, NASA Grant NAG5-9717, NOAA Grant PID-2207021, and Grant NA03OAR4310096. This research was partially developed during the author's first and second visits to the University of Utah. The authors thank the anonymous reviewers for their suggestions that helped improve the manuscript. Thanks also go to D. Vila for his valuable assistance with the FORTRACC program and D. Allured for his assistance in providing GDAS data.

REFERENCES

Augustine, J. A., and K. W. Howard, 1988: Mesoscale convective complexes over the United States during 1985. *Mon. Wea. Rev.,* **116,** 685–701.

Berbery, H., and E. Collini, 2000: Springtime precipitation and water vapor flux over southeastern South America. *Mon. Wea. Rev.,* **128,** 1328–1346.

——, and V. Barros, 2002: The hydrologic cycle of the La Plata Basin in South America. *J. Hydrometeor.,* **3,** 630–645.

Campetella, C., and C. Vera, 2002: The influence of the Andes Mountains on the South American low level flow. *Geophys. Res. Lett.,* **29,** 1826, doi:10.1029/2002GL015451.

Cohen, J. C. P., M. A. F. Silva Dias, and C. A. Nobre, 1995: Environmental conditions associated with Amazonian squall lines: A case study. *Mon. Wea. Rev.,* **123,** 3163–3174.

Cotton, W. R., M. S. Lin, R. L. McAnelly, and C. J. Tremback, 1989: A composite model of mesoscale convective complexes. *Mon. Wea. Rev.,* **117,** 765–783.

Douglas, M. W., M. Nicolini, and C. Saulo, 1998: Observational evidences of a low level jet east of the Andes during January–March 1998. *Meteorologica,* **23,** 63–72.

Fritsch, J. M., and G. S. Forbes, 2001: Mesoscale convective systems. *Severe Convective Storms, Meteor. Monogr.,* No. 50, Amer. Meteor. Soc., 323–356.

Janowiak, J., R. Joyce, and Y. Yarosh, 2001: A real-time global half hourly pixel resolution infrared dataset and its applications. *Bull. Amer. Meteor. Soc.,* **82,** 205–217.

Johnson, R., and B. E. Mapes, 2001: Mesoscale processes and severe convective weather. *Severe Convective Storms, Meteor. Monogr.,* No. 50, Amer. Meteor. Soc., 71–122.

Liebmann, B., G. N. Kiladis, C. Vera, A. C. Saulo, and L. M. V. Carvalho, 2004: Subseasonal variations of rainfall in South America in the vicinity of the low-level jet east of the Andes and comparison to those in the South Atlantic convergence zone. *J. Climate,* **17,** 3829–3842.

Machado, L. A. T., and H. Laurent, 2004: The convective system

area expansion over Amazonia and its relationships with convective system life duration and high-level wind divergence. *Mon. Wea. Rev.,* **132,** 714–725.

——, W. B. Rossow, R. L. Guedes, and A. W. Walker, 1998: Life cycle variations of mesoscale convective systems over the Americas. *Mon. Wea. Rev.,* **126,** 1630–1654.

Maddox, R. A., 1983: Large-scale meteorological conditions associated with midlatitude, mesoscale convective complexes. *Mon. Wea. Rev.,* **111,** 1475–1493.

Marengo, J. A., M. W. Douglas, and P. L. Silva Dias, 2002: The South American low level jet east of the Andes during the 1999 LBATRMM and LBA-WET AMC campaign. *J. Geophys. Res.,* **107,** 8079, doi:10.1029/2001JD001188.

——, W. R. Soares, C. Saulo, and M. Nicolini, 2004: Climatology of the low level jet east of the Andes as derived from the NCEP–NCAR reanalyses: Characteristics and temporal variability. *J. Climate,* **17,** 2261–2280.

Mota, G. V., 2003: Characteristics of rainfall and precipitation features defined by the Tropical Rainfall Measuring Mission over South America. Ph.D. dissertation, University of Utah, 215 pp.

Nesbitt, S. W., E. J. Zipser, and D. J. Cecil, 2000: A census of precipitation features in the Tropics using TRMM: Radar, ice scattering, and lightning observations. *J. Climate,* **13,** 4087–4106.

Nicolini, M., and A. C. Saulo, 2000: ETA characterization of the 1997–98 warm season Chaco jet cases. Preprints, *Sixth Int. Conf. on Southern Hemisphere Meteorology and Oceanography,* Santiago, Chile, Amer. Meteor. Soc., 330–331.

——, and ——, 2006: Modeled Chaco low-level jets and related precipitation patterns during the 1997–1998 warm season. *Meteor. Atmos. Phys.,* **94,** 129–143.

——, K. M. Waldron, and J. Paegle, 1993: Diurnal oscillations of low-level jets, vertical motion, and precipitation: A model case study. *Mon. Wea. Rev.,* **121,** 2588–2610.

——, C. Saulo, J. C. Torres, and P. Salio, 2002: Strong South American low level jet events characterization during warm season and implications for enhanced precipitation. *Meteorologica,* **27** (1–2), 59–69.

——, P. Salio, G. Ulke, J. Marengo, M. Douglas, J. Paegle, and E. Zipser, 2004: South American low level jet diurnal cycle and three dimensional structure. *CLIVAR Exchanges,* No. 9, International CLIVAR Project Office, Southampton, United Kingdom, 6–8.

Nieto Ferreira, R., T. M. Rickenbach, D. L. Herdies, and L. M. V. Carvalho, 2003: Variability of South American convective cloud systems and tropospheric circulation during January–March 1998 and 1999. *Mon. Wea. Rev.,* **131,** 961–973.

Nogués-Paegle, J., and K. C. Mo, 1997: Alternating wet and dry conditions over South America during summer. *Mon. Wea. Rev.,* **125,** 279–291.

Paegle, J., 2000: American low level jets in observation and theory: The ALLS project. Preprints, *Sixth Int. Conf. on Southern Hemisphere Meteorology and Oceanography,* Santiago, Chile, Amer. Meteor. Soc., 161–162.

Salio, P., 2002: Characterization of extreme low level jet events east of the Andes using reanalysis (in Spanish). Ph.D. thesis, University of Buenos Aires, 231 pp.

——, M. Nicolini, and A. C. Saulo, 2002: Chaco low level jet events characterization during the austral summer season by ERA reanalysis. *J. Geophys. Res.,* **107,** 4816, doi:10.1019/2001JD001315.

——, E. J. Zipser, M. Nicolini, and C. Liuct, 2004: Diurnal cycle of mesoscale convective systems over Southeastern South America. Preprints, *14th Int. Precipitation and Cloud Conf.,* Bologna, Italy, International Association of Meteorology and Atmospheric Science, 1844–1847.

Saulo, C. A., M. Seluchi, and M. Nicolini, 2004: A case study of a Chaco low-level jet event. *Mon. Wea. Rev.,* **132,** 2669–2683.

Silva Dias, M. A. F., 1999: Storms in Brazil. *Hazards and Disasters Series—Storms,* R. Pielke Sr. and R. Pielke Jr., Eds., Vol. II, Routledge, 207–219.

Siqueira, J. R., and L. A. T. Machado, 2004: Influence of the frontal systems on the day-to-day convection variability over South America. *J. Climate,* **17,** 1754–1766.

Velasco, I. Y., and J. M. Fritsch, 1987: Mesoscale convective complexes in the Americas. *J. Geophys. Res.,* **92,** 9591–9613.

Vera, C., P. K. Vigliarolo, and E. H. Berbery, 2002: Cold season synoptic-scale waves over subtropical South America. *Mon. Wea. Rev.,* **130,** 684–699.

——, and Coauthors, 2006: The South American Low-Level Jet Experiment. *Bull. Amer. Meteor. Soc.,* **87,** 63–77.